



Heterogeneous bimetallic Au–Co nanoparticles as new efficient catalysts for the three-component coupling reactions of amines, alkynes and CH_2Cl_2

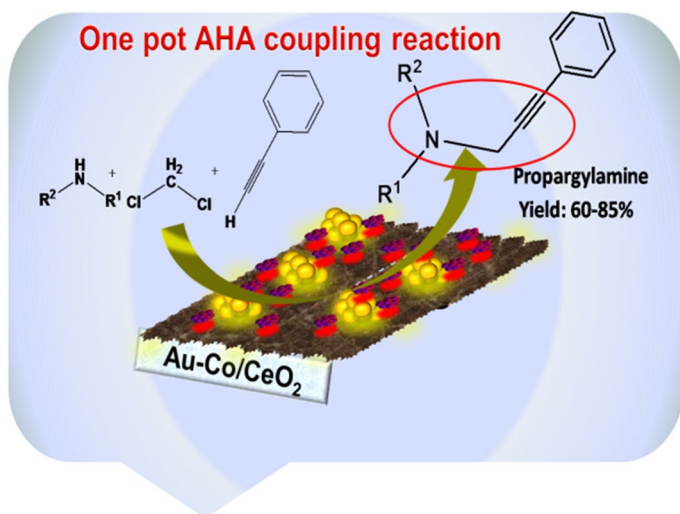
A. Berrichi^{1,4} · R. Bachir¹ · S. Bedrane¹ · N. Choukchou-Braham¹ · K. Belkacemi^{2,3}

Received: 20 December 2018 / Accepted: 11 March 2019 / Published online: 27 March 2019
© Springer Nature B.V. 2019

Abstract

Propargylamines are key intermediates for the synthesis of many biologically active molecules. A new synthesis of propargylamines via a three component-coupling reactions of amines, alkynes and dichloromethane (AHA) using bimetallic nanoparticles Au–M (M = Cr, Cu, Co) supported on CeO_2 catalysts was investigated. Bimetallic particles are regularly distributed on ceria and range in size from 8 to 11 nm. Synergetic effect between gold and the second metal was demonstrated. Different propargylamines were synthesized with high yields (60–85%) using Au–Co/ CeO_2 as an active heterogeneous catalyst.

Graphical abstract



Keywords Three component-coupling · Gold · Bimetallic · Heterogeneous · Nanoparticles

Introduction

Propargylamines are key intermediates for the synthesis of many biologically active nitrogen molecules such as β -lactams and therapeutic drugs [1–4].

Moreover, some propargylamines are known to be neurodegenerative protecting groups. Rasagiline and Deprenyl are used in the treatment of dementia diseases such as the Parkinson [5–9].

These propargylamines are often synthesized by three-component coupling reactions of alkynes, amines, and a source of active methylene [10]. This way is called A3 multicomponent reaction when aldehydes are used as a methylene source. Such reactions can be catalyzed by gold nanoparticles [11–19].

Another strategy to synthesize propargylamines involves the activation of the C–H bond of an alkyne and the C–X bond of a dihalomethane. This is a three-component coupling reaction of an alkyne, a dihalomethane and an amine. This way is called AHA multicomponent reaction. These coupling reactions are mainly catalyzed by metal salts in homogeneous conditions with CuCl [20], CoBr₂ [21], In₂O₃ [22], FeCl₃ [23], K[AuCl₄] [24], Ni ligands [25], silver salts [26] but few heterogeneous catalysts have been used [27, 28].

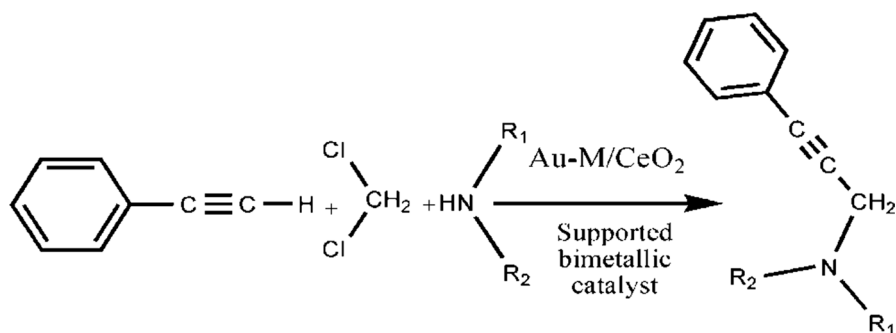
Gold nanoparticles deposited on reducible supports such as Fe₂O₃, CeO₂, and TiO₂ have shown good activities in various reactions [29–33]. However, supported gold bimetallic catalysts are not widely used. In addition, the majority of supported bimetallic catalysts cited in the literature relate to the association of gold to noble metals Au–Pd [34–37], Au–Pt [38–40], Au–Ag [41–44] and only a couple of publications report the association of gold to transition metals and gold Au–Fe [45], Au–Co [46]. Furthermore, these catalysts have never been used for multicomponent coupling reactions and particularly for the synthesis of propargylamines by the AHA way.

In this paper, we report the synthesis of different propargylamines via a one-pot three-component coupling reaction of phenylacetylene, dichloromethane and amines (AHA) using different Au–M/CeO₂ (M=Cu, Cr, Co) nanoparticles (Scheme 1). A special consideration is given to Au–Co/CeO₂. The catalysts are prepared by co-DPU.

Experimental

Materials

HAuCl₄·3H₂O, Co(NO₃)₂·6H₂O, Cr(NO₃)₃·9H₂O, Cu(NO₃)₂·3H₂O, CO(NH₂)₂, AgNO₃, NaBH₄, and commercial ceria nano-powder (nanoparticles sizes \leq 20 nm) were purchased from Sigma Aldrich.



Scheme 1 AHA coupling reaction of phenylacetylene, dichloromethane and amines

Catalysts preparation

The monometallic 1% Au/CeO₂ catalyst is prepared by deposition precipitation with urea (DPU) as described elsewhere [27, 45, 47]. Bimetallic catalysts 1% Au–1% M/CeO₂ are prepared using a one pot co-deposition precipitation with the urea (CO-DPU) method. Gold salt and the second metal salt are added on the support at the same time. The mixture is heated up to 80 °C and kept under agitation for 16 h. Finally, the materials are dried at 120 °C overnight.

Characterization

Diffuse reflectance DRUV–Vis spectroscopy measurements were carried out at room temperature on a Lambda 800 UV–Vis spectrometer in the range of 200–800 nm. This setup was equipped with a diffuse reflectance accessory set to collect the diffuse reflected light only. BaSO₄ was used as standard.

The BET surface areas were determined from N₂ adsorption isotherms at 77 K using a Quantachrom NOVA 1000 instrument. The catalyst was outgazed in situ at 250 °C for 10 h.

FTIR spectra were recorded using a Thermo Nicolet Nexus 670 spectrometer in absorbance mode at 32 scans with a resolution of 4 cm^{−1}.

Transmission electron microscopy (TEM) micrographs were collected on a JEOL JEM-1230 electron microscope.

AHA coupling

A mixture of phenylacetylene (2 mmol), amine (2.2 mmol), CH₂Cl₂ (1.5 mmol), DABCO (2 mmol), catalyst (80 mg) and 3 mL of CH₃CN (solvent) are loaded in a sealed reaction 10 mL- vial. After stirring at 65 °C for 24 h, the reaction mixture is diluted with H₂O, extracted with CH₂Cl₂, dried over Na₂SO₄ and concentrated by evaporation of solvent. This step gives the crude product, which is further purified

by column chromatography on silica gel (acetate/hexane) to afford the corresponding propargylic amine [27].

Reaction sample analysis

^1H and ^{13}C NMR spectra were recorded on a Varian Mercury 400 NMR spectrometer at operating frequencies of 400 and 100 MHz, respectively, in CDCl_3 as solvent.

Gas chromatography–mass spectrometry (GC–MS) was performed with a Shimadzu GC-2010 coupled with a GCMSQP2010. The products are known in the literature.

***N,N*-Diethyl-3-phenylprop-2-yn-1-amine** ^1H NMR (400 MHz, CDCl_3) (δ ppm): 1.10–1.136 (t, 6H, 2 CH_3), 2.60–2.66 (q, 4H, 2 CH_2), 3.643 (s, 2H, CH_2), 7.27–7.30 (m, 3 H_{ar}), 7.41–7.43 (m, 2 H_{ar});

^{13}C NMR (100 MHz, CDCl_3) (δ ppm): 11.61(2C), 40.44(1C), 46.31(2C), 83.34(1C), 83.96(1C), 122.35(1C), 126.89(2C), 127.20 (1C), 130.69 (2C);

MS: m/z = 188.089, 115.027 ($-\text{HN}(\text{CH}_2\text{CH}_3)_2$),

IR (ν , cm^{-1}) = 760, 689, 1198, 1320.

4-(3-phenylprop-2-ynyl) morpholine ^1H NMR (400 MHz, CDCl_3) (δ ppm): 2.62–2.64 (t, 4 $\text{H}_{\text{morpholine}}$), 3.74–3.77 (t, 4H), 3.54 (s, 2H), 7.28–7.29 (m, 3 H_{ar}), 7.41–7.43 (m, 2 H_{ar});

^{13}C NMR (100 MHz, CDCl_3) (δ ppm): 48.04(1C), 52.45(2C), 66.90(2C), 84.09(1C), 85.58(1C), 122.98(1C), 128.17(2C), 128.26(1C), 131.71(2C).

MS (m/z): 100.115 (-102 , morpholine- CH_2), 115.0975 (-87 , morpholine), 202.1932 (100%, $\text{M} + \text{H}$);

IR (ν , cm^{-1}) = 690, 754, 1120, 1288, 1346, 1452, 1489, 1598, 2959, 3056.

1-(3-phenylprop-2-ynyl)pyrrolidine ^1H NMR (400 MHz, CDCl_3) (δ ppm): 1.820–1.840 (q, 4 $\text{H}_{\text{pyrrolidine}}$), 2.77–2.800 (t, 4 $\text{H}_{\text{pyrrolidine}}$), 3.67 (s, 2H, CH_2), 7.210–7.250 (dd, H_{ar}), 7.371–7.395 (m, H_{ar});

^{13}C NMR (100 MHz, CDCl_3) (δ ppm): 23.89(2C), 43.70(1C), 52.48(2C), 83.79(1C), 85.39(1C), 122.82(1C), 128.3(3C), 131.77 (2C);

IR (ν , cm^{-1}) = 675, 866, 1123, 1265, 1508, 1642, 1684, 2346, 2933.

1-(3-phenylprop-2-ynyl)piperidine ^1H NMR (CDCl_3 , 250 MHz) (δ ppm): 1.38–1.46(m, 6 $\text{H}_{\text{piperidine}}$), 1.60–1.63 (m, 4 $\text{H}_{\text{piperidine}}$), 3.45 (s, 2H), 7.25–7.26(t, 2 H_{ar}), 7.39–7.42 (m, 3 H_{ar});

^{13}C NMR (CDCl_3 , 62.9 MHz) (δ ppm): 23.94(1C), 30.95(1C), 48.49(2C), 53.47(2C), 85.02(1C), 85.03(1C), 123.30(1C), 127.98(2C), 128.22(1C), 131.72(2C).

IR (ν , cm^{-1}) = 695, 753, 1158, 1366, 1452, 1736, 2347, 2800, 2804, 2943.

Results and discussion

DRUV–Vis characterization

The DRUV–Vis spectra of CeO_2 , 1%Au/ CeO_2 , 1%Au–1%Cu/ CeO_2 , 1%Au–1%Co/ CeO_2 and 1%Au–1%Cr/ CeO_2 are shown in Fig. 1. The DRUV–Vis characteristic bands of the different catalysts determined after deconvolution of the respective spectra are summarized in Table 1. Ceria (Fig. 1a) shows a band at 216 nm corresponding to the charge transfer of O^{2-} to Ce^{4+} and two other bands at 269 nm and 310 nm corresponding to the charge transfer of oxygen to cation species in a lower oxidative state [48]. These bands are also observable for 1%Au/ CeO_2 (Fig. 1b). Nevertheless they are shifted to higher values (269 nm 275 nm; 310 nm 321 nm) indicating metal–support interactions. Moreover, the 1%Au/ CeO_2 spectrum presents a new band at 553 nm. This band is characteristic of gold nanoparticles surface plasmon resonance. In the case of the bimetallic catalysts, a net shift of the ceria characteristic bands can be observed. The gold nanoparticles surface plasmon resonance bands appear at 514 nm for Au–Co/ CeO_2 (Fig. 1c), 537 nm for Au–Cr/ CeO_2 (Fig. 1d) and 516 nm for Au–Cu/ CeO_2 (Fig. 1e) respectively.

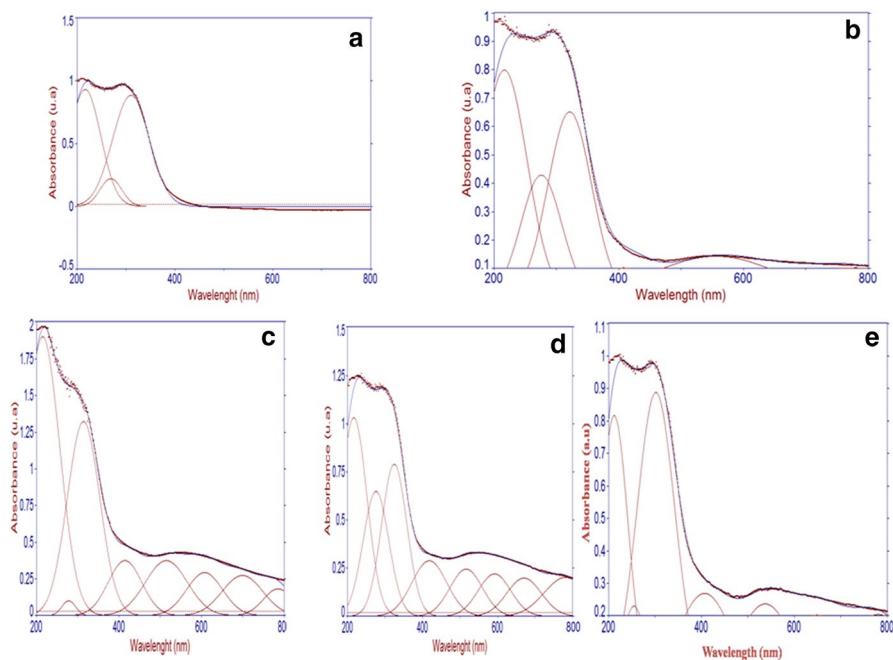


Fig. 1 DRUV–Vis spectra of **a** CeO_2 , **b** 1%Au/ CeO_2 , **c** 1%Au–1%Co/ CeO_2 , **d** 1%Au–1%Cu/ CeO_2 , **e** 1%Au–1%Cr/ CeO_2

Table 1 DRUV–Vis characteristic bands of the different catalysts

Catalyst	Peak center	Peak area	Interpretation	References	
CeO ₂	216	74	Charge transfer of O ²⁻ to Ce ⁴⁺	[49]	
	269	12	Charge transfer of oxygen to cation species in lower oxidative state		
	310	83			
1%Au/CeO ₂	216	72	Ceria characteristic bands	[47, 50, 51]	
	275	34			
	321	57			
	556	36			Gold nanoparticle surface plasmon resonance band
1%Au–1%Co/CeO ₂	215	197	Ceria characteristic bands	[52–56]	
	277	4			
	314	131			
	514	47			Gold nanoparticle surface plasmon resonance band
	414	38	Characteristic bands of Co ³⁺ and Co ²⁺ species		
	607	32			
	699	33			
	785	16			
1%Au–1%Cu/CeO ₂	216	90	Ceria characteristic bands	[57–60]	
	275	56			
	324	67	Gold nanoparticle surface plasmon resonance band		
	516	26			
	418	33	Characteristic bands of Cu ²⁺		
	592	24			
	671	23			
	781	28			
1%Au–1%Cr/CeO ₂	212	60		Ceria characteristic bands	[61–64]
	254	13			
	302	89			
	537	33	Gold nanoparticle surface plasmon resonance band		
	407	37	Characteristic bands of Cr ³⁺ , Cr ⁶⁺ and Cr ⁵⁺		
	649	29			
	781	33			

The gold nanoparticles surface plasmon resonance band shift from 553 nm in Au/CeO₂ to lower values in the bimetallic catalysts could be explained by an interaction between Au and the second metal. Furthermore, different bands corresponding to different transitions in Cu, Co and Cr ions are shown.

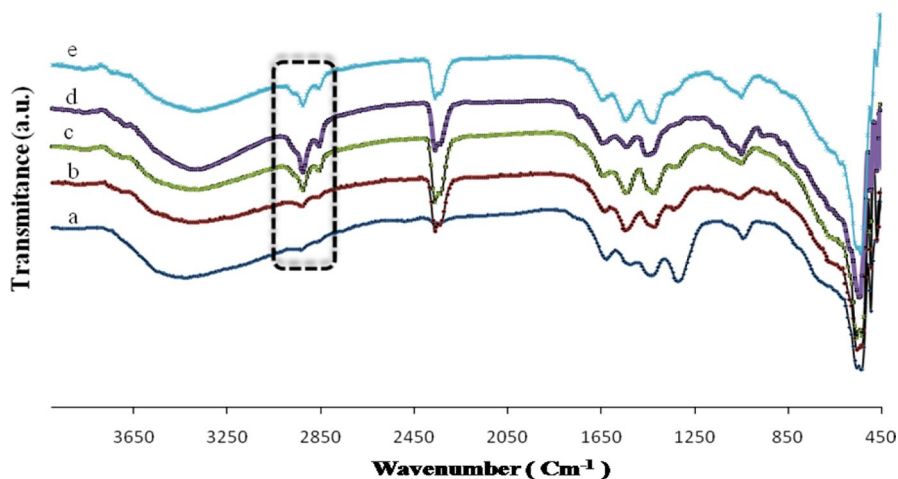


Fig. 2 FTIR spectra of **a** CeO₂, **b** 1%Au/CeO₂, **c** 1%Au–1%Co/CeO₂, **d** 1%Au–1%Cu/CeO₂, **e** 1%Au–1%Cr/CeO₂

Table 2 BET surface area of the different catalysts

Catalyst	BET surface area (m ² g ⁻¹)	Total pore volume (cm ³ g ⁻¹)
1%Au/CeO ₂	70	0.142
1%Au–1%Cu/CeO ₂	47	0.126
1%Au–1%Co/CeO ₂	64	0.124
1%Au–1%Cr/CeO ₂	64	0.123

FTIR characterization

FTIR spectra of the support as well as monometallic and bimetallic catalysts are shown in Fig. 2. A band at 1050 cm⁻¹ related to the stretching vibration of C–O in carbonates [65] and bands at 1250–1750 cm⁻¹ assignable to the OCO asymmetric and symmetric stretching vibrations are shown in the case of CeO₂ and Au/CeO₂ [66]. For the bimetallic catalysts the band in 2300–2350 cm⁻¹ is attributed to CO₂ (Fig. 2d–f) [67]. Two new bands are situated at 2800–3000 cm⁻¹ related to CH₃ vibration and adsorbed water [67, 68].

N₂-physisorption characterization

Nitrogen adsorption and desorption isotherms were recorded for monometallic and bimetallic catalysts. The corresponding textural parameters are shown in Table 2. No significant modification in BET surface area was noted by adding

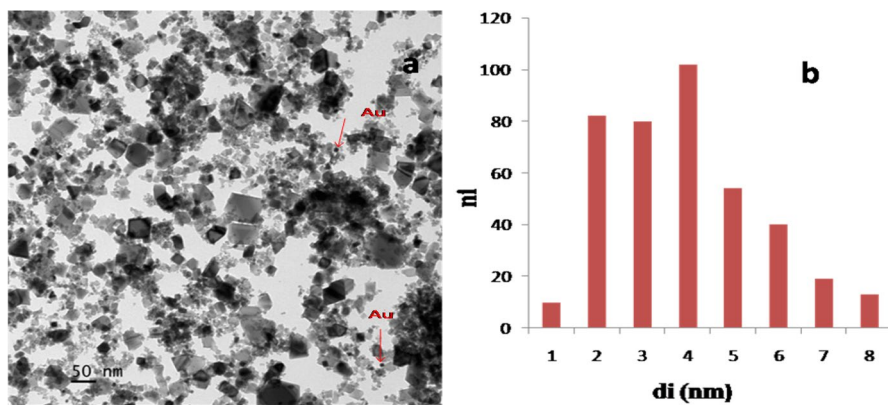


Fig. 3 TEM characterization of 1%Au/CeO₂ **a** TEM image and **b** size distribution histogram

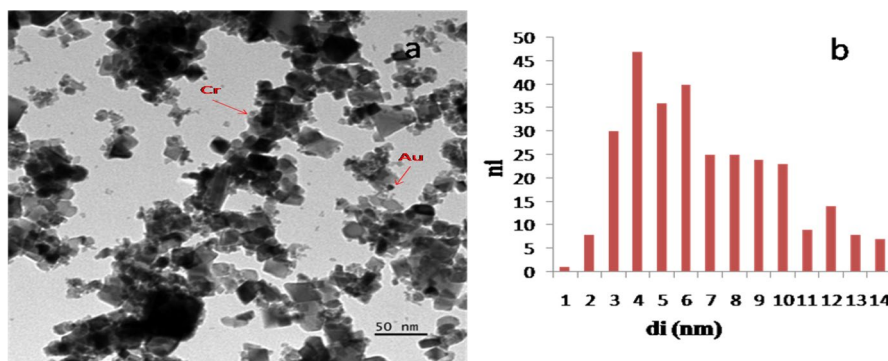


Fig. 4 TEM characterization of 1%Au-1%Cr/CeO₂ **a** TEM image and **b** size distribution histogram

Cr or Co to the monometallic 1%Au/CeO₂ catalyst. However, Cu induces ~33% decrease of this surface area.

TEM characterization

The Au and Au-M particles are nanosized (Figs. 3, 4, 5, 6). The histogram of the particle size distribution for Au/CeO₂ catalyst has a Gaussian shape (Fig. 3b). The majority of the gold particles range from 2 to 4 nm with a mean size of 4.8 nm. The addition of the second metal induces an increase in the particles average size up to 11 nm in the case of Cr (Fig. 4), 9 nm the case of Cu (Fig. 5) and 8 nm the case of Co (Fig. 6).

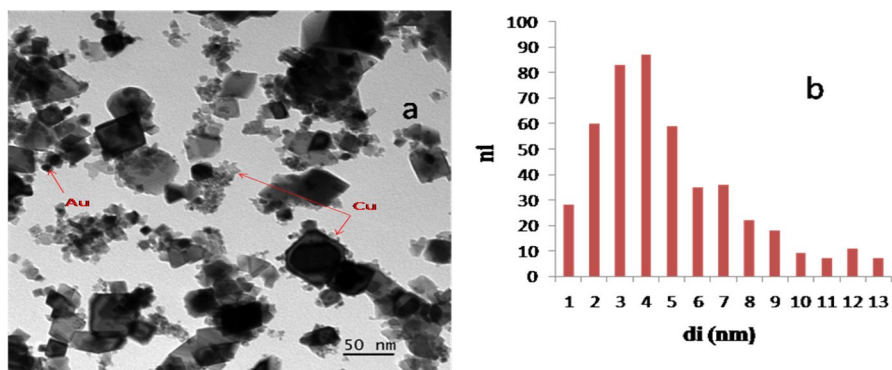


Fig. 5 TEM characterization of 1%Au–1%Cu/CeO₂ **a** TEM image and **b** size distribution histogram

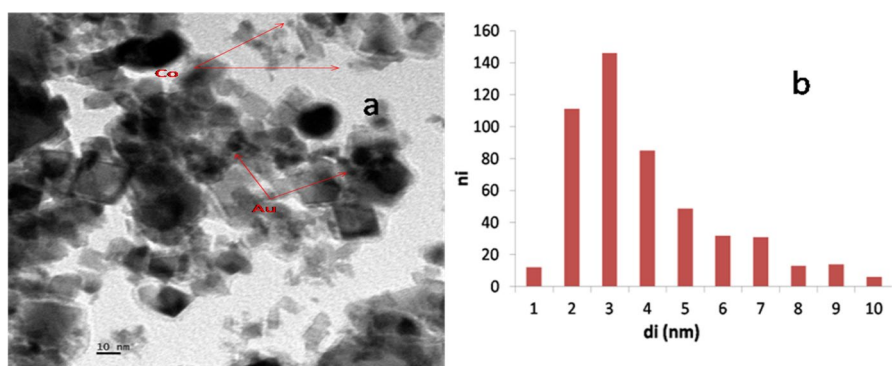
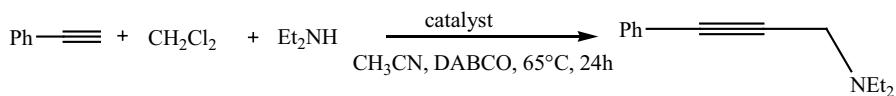


Fig. 6 TEM characterization of 1%Au–1%Co/CeO₂ **a** TEM image and **b** size distribution histogram

Table 3 Three-component coupling reaction of phenylacetylene, CH₂Cl₂ and diethylamine over 1% Au/CeO₂ and 1%Au–1%M/CeO₂ (M=Cr, Cu, Co)



Entries	Catalysts	Yield (%)	TON
1	CeO ₂	0	0
2	1%Au/CeO ₂	23	114
3	1%Au–1%Cr/CeO ₂	30	150
4	1%Au–1%Cu/CeO ₂	42	210
5	1%Au–1%Co/CeO ₂	57	284

Catalyst activity in AHA coupling

The results of the three-component coupling reaction of diethylamine, dichloromethane, phenylacetylene (AHA) using mono and bimetallic catalysts are shown in Table 3. The bimetallic catalysts are more active than the monometallic one. They reached 30–57% yield (entries 3, 4, 6). The monometallic catalyst registered only 23% (entry 2) while ceria was completely inactive (entry 1). These results indicate a positive synergistic effect between gold and the second metal.

As Co gave the best improvement for the activity of gold nanoparticles, we investigated the influence of its content on the catalytic performance. Different bimetallic catalysts 1%Au–x%Co/CeO₂, where x was varied from 1 to 4%, were prepared and tested. The 1%Co/CeO₂ and 1%Au/CeO₂ were also prepared for comparison purposes.

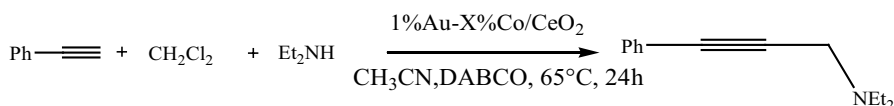
As highlighted in Table 4, increasing the Co loading in the bimetallic catalyst increased markedly the reaction yield. We confirm, thus, the effect of cobalt to improve the activity of gold nanoparticles. Indeed, by increasing Co content, the yield of propargylamine increases (Table 4).

The yield obtained with the bimetallic catalysts remains significantly higher than the sum of yields obtained with the two monometallic catalysts, for all cases. For instance, the yield obtained with 1%Au–1%Co/CeO₂ is circa two folds higher than that obtained with two monometallic catalysts.

$$\frac{\text{Yield}(1\% \text{Au} - 1\% \text{Co}/\text{CeO}_2)}{\text{Yield}(1\% \text{Au}/\text{CeO}_2) + \text{Yield}(1\% \text{Co}/\text{CeO}_2)} = \frac{57}{23 + 10} = 1.7$$

$$\frac{\text{TON}(1\% \text{Au} - 1\% \text{Co}/\text{CeO}_2)}{\text{TON}(1\% \text{Au}/\text{CeO}_2) + \text{TON}(1\% \text{Co}/\text{CeO}_2)} = \frac{284}{14 + 114} = 2.2$$

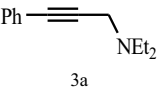
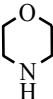
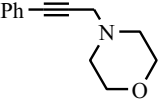
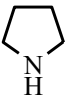
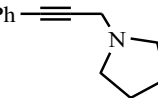
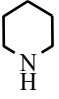
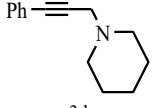
Table 4 Three-component coupling reaction of phenylacetylene, CH₂Cl₂ and diethylamine catalyzed over 1%Au–x%Co/CeO₂ (x=0–4%)



Entries	Catalysts	Yield (%)	TON
1	1%Co/CeO ₂	10	14
2	1%Au/CeO ₂	23	114
3	1%Au–1%Co/CeO ₂	57	284
4	1%Au–2%Co/CeO ₂	62	310
5	1%Au–4%Co/CeO ₂	70	350

Table 5 Synthesis of different propargylamines catalyzed by 1%Au–4%Co/CeO₂

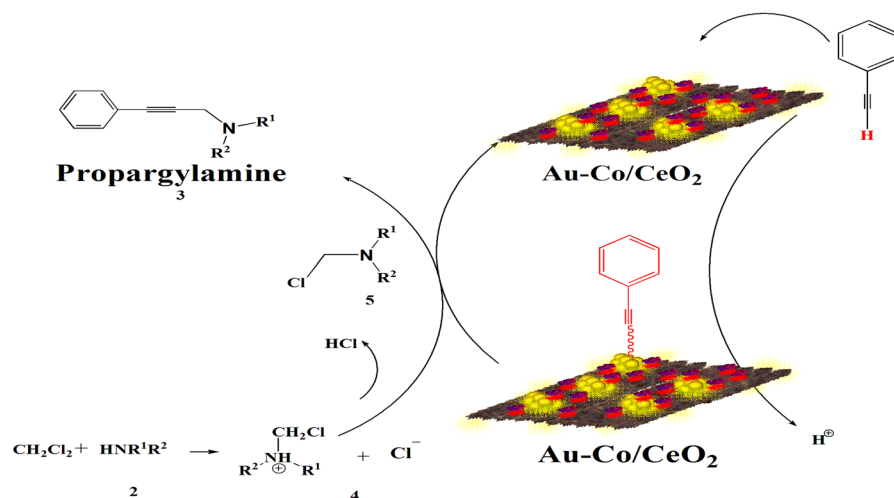
$$\text{Ph}-\text{C}\equiv\text{C}-\text{H} + \text{CH}_2\text{Cl}_2 + \text{HNR}_1\text{R}_2 \xrightarrow[\text{CH}_3\text{CN, DABCO, 65 }^\circ\text{C, 24 h}]{1\% \text{Au}-4\% \text{Co}/\text{CeO}_2} \text{Ph}-\text{C}\equiv\text{C}-\text{CH}_2-\text{NR}_1\text{R}_2$$

	1a	2a-2d		3a-3d		
Entry	Amine	Propargylamine	Yield	Yield 2%Au/CeO ₂ [27]	TON	TON [27]
1	Et ₂ NH 2a	 3a	70	53	350	132
2	 2b	 3b	85	55	424	138
3	 2c	 3c	67	53	334	132
4	 2d	 3d	60	59	300	148

The association of gold nanoparticles and cobalt induces a positive synergistic effect for the AHA coupling reaction.

Finally, we used various secondary amines (2a–d) while keeping phenylacetylene as a terminal alkyne. The 1%Au–4%Co/CeO₂ was used as a catalyst for this study. Different propargylamines were synthesized with high yields (67–85%) (Table 5).

We compared the yields obtained in this study for the different propargylamines with those obtained using 80 mg of a monometallic catalyst 2%Au/CeO₂ published elsewhere [27]. In all cases the yields obtained with bimetallic catalyst are higher than those obtained with the monometallic catalyst (Table 5). This confirms the positive synergy between Au and Co.



Scheme 2 Plausible mechanism for the AHA coupling reactions over Au-Co/CeO₂

Mechanism

In a previous study [27] we have proposed a mechanism for this reaction using a monometallic catalyst Au/CeO₂. We still think that this mechanism is plausible in the case of the bimetallic catalyst (Scheme 2). Indeed, in this mechanism we suggested a reaction of an adsorbed phenyl acetylene and a chloro-N,N-dimethylmethanamine. This chloro-N,N-dimethylmethanamine is produced by a reaction between the amine and the CH₂Cl₂ via the formation of a chloro-N,N-dimethylmethanaminium chloride salt.

Conclusion

In this work, we have prepared nanosupported bimetallic catalysts Au-M/CeO₂ (M = Cr, Cu, Co). Bimetallic particles are regularly distributed on ceria with sizes ranging from 8 to 11 nm. The particles size depends on the nature of the second metal. Furthermore, DRUV-Vis spectroscopy and FTIR showed that the CO-DPU preparation method used in this work leads to a close interaction between gold and the second metal. These interactions make gold NPs more stable and more active in the bimetallic catalysts. Indeed, bimetallic catalysts are very active in the three-component coupling reaction AHA. The activity of bimetallic catalysts is always higher than the monometallic one. However, this activity depends on the nature of the second metal. We have established the following increasing order activity Au-Cr/CeO₂ < Au-Cu/CeO₂ < Au-Co/CeO₂. In the case of Au-Co/CeO₂ we have demonstrated a synergetic effect between the Au and Co.

As Au–Co/CeO₂ is the most active catalyst, we chose it to synthesize various propargylamines by varying the starting amine. Indeed, we have synthesized several propargylamines with good yields (60–85%). This study showed the possibility of enhancing the stability and the activity of Au NPs by adding a transition metal (Cr, Co, Cu) using the CO-DPU method. In the other hand, this study has opened up a new method to synthesize propargylamines by AHA with very active heterogeneous bimetallic catalysts.

Acknowledgements We thank DGRDST and the University of Tlemcen for funding this work.

References

1. I. Bolea, A. Gella, M. Unzeta, J. Neural Transm. **120**, 893 (2013)
2. I. Matsuda, J. Sakakibara, H. Nagashima, Tetrahedron Lett. **32**, 7431 (1991)
3. M.B.H. Youdim, L. Kupersmidt, T. Amit, O. Weinreb, Parkinsonism Relat. Disord. **20**, 132 (2014)
4. G. Abbiati, A. Arcadi, G. Bianchi, S. Di Giuseppe, F. Marinelli, E. Rossi, J. Org. Chem. **68**, 6959 (2003)
5. M.A. Huffman, N. Yasuda, A.E. DeCamp, E.J.J. Grabowski, J. Org. Chem. **60**, 1590 (1995)
6. J.J. Chen, D.M. Swope, J. Clin. Pharmacol. **45**, 878 (2005)
7. O. Bar-Am, O. Weinreb, T. Amit, M.B.H. Youdim, Faseb J. **19**, 1899 (2005)
8. W. Maruyama, Y. Akao, M.B. Youdim, B.A. Davis, M. Naoi, J. Neurochem. **78**, 727 (2001)
9. M. Yogev-Falach, T. Amit, O. Bar-Am, M.B.H. Youdim, Faseb J. **17**, 2325 (2003)
10. N. Bahri-Laleh, S. Sadjadi, Res. Chem. Intermed. **44**, 6351 (2018)
11. G. Villaverde, A. Corma, M. Iglesias, F. Sánchez, ACS Catal. **2**, 399 (2012)
12. X. Zhang, A. Corma, Angew. Chem. Int. Ed. **47**, 4358 (2008)
13. M. Gonzalez-Bejar, K. Peters, G.L. Hallett-Tapley, M. Grenier, J.C. Scaiano, Chem. Commun. **49**, 1732 (2013)
14. B. Karimi, M. Gholinejad, M. Khorasani, Chem. Commun. **48**, 8961 (2012)
15. L. Liu, X. Zhang, J. Gao, C. Xu, Green Chem. **14**, 1710 (2012)
16. Y. Chen, C. Liu, H. Abroshan, Z. Li, J. Wang, G. Li, M. Haruta, J. Catal. **340**, 287 (2016)
17. S. Shabbir, Y. Lee, H. Rhee, J. Catal. **322**, 104 (2015)
18. L.L. Chng, J. Yang, Y. Wei, J.Y. Ying, Adv. Synth. Catal. **351**, 2887 (2009)
19. L. Abahmane, J.M. Köhler, G.A. Groß, Chem. Eur. J. **17**, 3005 (2011)
20. Z. Lin, D. Yu, Y. Zhang, Tetrahedron Lett. **52**, 4967 (2011)
21. Y. Tang, T. Xiao, L. Zhou, Tetrahedron Lett. **53**, 6199 (2012)
22. M. Rahman, A.K. Bagdi, A. Majee, A. Hajra, Tetrahedron Lett. **52**, 4437 (2011)
23. J. Gao, Q.W. Song, L.N. He, Z.Z. Yang, X.Y. Dou, Chem. Commun. **48**, 2024 (2012)
24. D. Aguilar, M. Contel, E.P. Urriolabeitia, Chem-Eur. J. **16**, 9287 (2010)
25. S.R. Lanke, B.M. Bhanage, Appl. Organomet. Chem. **27**, 729 (2013)
26. X. Chen, T. Chen, Y. Zhou, C.T. Au, L.B. Han, S.F. Yin, Org. Biomol. Chem. **12**, 247 (2014)
27. A. Berrichi, R. Bachir, M. Benabdallah, N. Choukchou-Braham, Tetrahedron Lett. **56**, 1302 (2015)
28. R.K. Sharma, S. Sharma, G. Gaba, RSC. Adv. **4**, 49198 (2014)
29. X. Liu, P. Guo, B. Wang, Z. Jiang, Y. Pei, K. Fan, M. Qiao, J. Catal. **300**, 152 (2013)
30. H.Z.S. Li, Z. Qina, G. Wang, Y. Zhang, Z. Wu, Z. Li, G. Chen, W. Dong, Z. Wu, L. Zheng, J. Zhang, T. Hu, J. Wang, Appl. Catal. B **144**, 498 (2014)
31. L. Delannoy, N. Weiher, N. Tsapatsaris, A.M. Beesley, L. Nchari, S.L.M. Schroeder, C. Louis, Top. Catal. **44**, 263 (2007)
32. L.F. Gutierrez, S. Hamoudi, K. Belkacemi, Appl. Catal. A **402**, 94 (2011)
33. S. Bedrane, C. Descorme, D. Duprez, Appl. Catal. A **289**, 90 (2005)
34. J. Long, H. Liu, S. Wu, S. Liao, Y. Li, ACS Catal. **3**, 647 (2013)
35. L. Zhang, A. Wang, J.T. Miller, X. Liu, X. Yang, W. Wang, L. Li, Y. Huang, C.Y. Mou, T. Zhang, ACS Catal. **4**, 1546 (2014)
36. N.E. Kolli, L. Delannoy, C. Louis, J. Catal. **297**, 79 (2013)

37. A. Cybula, J.B. Priebe, M.M. Pohl, J.W. Sobczak, M. Schneider, A. Zielińska-Jurek, A. Brückner, A. Zaleska, *Appl. Catal. B* **152**, 202 (2014)
38. C. Qiu, J. Zhang, H. Ma, *Solid State Sci.* **12**, 822 (2010)
39. S. Pal, G. De, *Phys. Chem. Chem. Phys.* **10**, 4062 (2008)
40. C.W. Chen, T. Serizawa, M. Akashi, *Chem. Mater.* **14**, 2232 (2002)
41. A. Sandoval, A. Aguilar, C. Louis, A. Traverse, R. Zanella, *J. Catal.* **281**, 40 (2011)
42. T. Benkó, A. Beck, K. Frey, D.F. Srankó, O. Geszti, G. Sáfrán, B. Maróti, Z. Schay, *Appl. Catal. A* **479**, 103 (2014)
43. P.M. More, D.L. Nguyen, M.K. Dongare, S.B. Umbarkar, N. Nuns, J.S. Girardon, C. Dujardin, C. Lancelot, A.S. Mamede, P. Granger, *Appl. Catal. B* **162**, 11 (2015)
44. A. Villa, D. Wang, D.S. Su, L. Prati, *Catal. Sci. Technol.* **5**, 55 (2015)
45. N. Ameer, A. Berrichi, S. Bedrane, R. Bachir, *Adv. Mater. Res.* **856**, 42 (2014)
46. X. Xu, Q. Fu, M. Wei, X. Wu, X. Bao, *Catal. Sci. Technol.* **4**, 3151 (2014)
47. N. Ameer, S. Bedrane, R. Bachir, A. Choukchou-Braham, *J. Mol. Catal. A Chem.* **374**, 1 (2013)
48. J. Saranya, K.S. Ranjith, P. Saravanan, D. Mangalaraj, R.T. Rajendra Kumar, *Mater. Sci. Semicond. Process.* **26**, 218 (2014)
49. P. Kaminski, M. Ziolek, *J. Catal.* **312**, 249 (2014)
50. P. Lakshmanan, P.P. Upare, N.-T. Le, Y.K. Hwang, D.W. Hwang, U.H. Lee, H.R. Kim, J.-S. Chang, *Appl. Catal. A* **468**, 260 (2013)
51. S. Padikkaparambil, B. Narayanan, Z. Yaakob, S. Viswanathan, S.M. Tasirin, *Int. J. Photoenergy* **2013**, 10 (2013)
52. T.A. Maia, J.M. Assaf, E.M. Assaf, *Fuel Process. Technol.* **128**, 134 (2014)
53. R. Palcheva, A. Spojakina, K. Jiratova, L. Kaluza, *Catal. Lett.* **137**, 216 (2010)
54. A. Mahroug, S. Boudjadar, S. Hamrit, L. Guerbous, *Struct. J. Mater. Sci.* **25**, 4967 (2014)
55. N. Rinaldi, T. Kubota, Y. Okamoto, *Ind. Eng. Chem. Res.* **48**, 10414 (2009)
56. N. Baliarsingh, K.M. Parida, G.C. Pradhan, *Ind. Eng. Chem. Res.* **53**, 3834 (2014)
57. A. Sandoval, C. Louis, R. Zanella, *Appl. Catal. B* **140**, 363 (2013)
58. X. Yuan, J. Zheng, Q. Zhang, S. Li, Y. Yang, J. Gong, *AIChE J.* **60**, 3300 (2014)
59. S. Derrouiche, H. Lauron-Pernot, C. Louis, *Chem. Mater.* **24**, 2282 (2012)
60. Y. Zhang, C. Chen, X. Lin, D. Li, X. Chen, Y. Zhan, Q. Zheng, *Int. J. Hydrogen Energy* **39**, 3746 (2014)
61. K. Kohler, M. Maciejewski, H. Schneider, A. Baiker, *J. Catal.* **157**, 301 (1995)
62. D. Tsukamoto, A. Shiro, Y. Shiraishi, T. Hirai, *J. Phys. Chem. C* **115**, 19782 (2011)
63. S. De Rossi, M. Pia Casaletto, G. Ferraris, A. Cimino, G. Minelli, *Appl. Catal. A* **167**, 257 (1998)
64. J. El-Idrissi, M. Kacimi, F. Bozon-Verduraz, M. Ziyad, *Catal. Lett.* **56**, 221 (1998)
65. B. Liu, C. Li, Y. Zhang, Y. Liu, W. Hu, Q. Wang, L. Han, J. Zhang, *Appl. Catal. B* **111**, 467 (2012)
66. X. Liu, P. Guo, B. Wang, Z. Jiang, Y. Pei, K. Fan, M. Qiao, *J. Catal.* **300**, 152 (2013)
67. I. Soykal, H. Sohn, S. Ozkan, *ACS Catal.* **2**, 2335 (2012)
68. B. Liu, C. Li, Y. Zhang, Y. Liu, W. Hu, Q. Wang, L. Han, J. Zhang, *Appl. Catal. B* **467**, 112 (2012)

Publisher's Note Springer Nature remains neutral with regard to jurisdictional claims in published maps and institutional affiliations.

Affiliations

A. Berrichi^{1,4} · R. Bachir¹ · S. Bedrane¹ · N. Choukchou-Braham¹ · K. Belkacemi^{2,3}

✉ A. Berrichi
berrichi.amina@yahoo.fr

✉ R. Bachir
redouane_bachir@hotmail.com

¹ Laboratory of Catalysis and Synthesis in Organic Chemistry, Université de Tlemcen, BP 119, Tlemcen, Algeria

- ² Department of Soil Sciences and Food Engineering, Université Laval, Quebec-City, QC G1V0A6, Canada
- ³ Centre in Green Chemistry and Catalysis (CGCC), 801 Sherbrooke Street West, Otto Maass Building, Room 416, Montreal, QC H3A 0B8, Canada
- ⁴ Institut of Sciences and Technologie, University center- Ain Témouchent, BP 284, 46000 Ain Témouchent, Algeria